

# Multi-harmonic cavity for suppressing surface pulsed heating

Cite as: AIP Conference Proceedings **1777**, 060003 (2016); <https://doi.org/10.1063/1.4965632>  
Published Online: 28 October 2016

Y. Jiang, and J. L. Hirshfield



View Online



Export Citation

## ARTICLES YOU MAY BE INTERESTED IN

### Multi-Harmonic Cavities for Increasing RF Breakdown Threshold

AIP Conference Proceedings **1299**, 324 (2010); <https://doi.org/10.1063/1.3520337>

### Study of the effect of loop inductance on the RF transmission line to cavity coupling coefficient

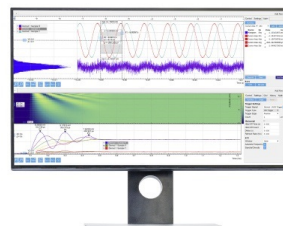
Review of Scientific Instruments **87**, 083308 (2016); <https://doi.org/10.1063/1.4961578>

### Structure-based, high transformer ratio collinear two-beam accelerator

AIP Conference Proceedings **1812**, 070003 (2017); <https://doi.org/10.1063/1.4975883>

## Challenge us.

What are your needs for  
periodic signal detection?



Zurich  
Instruments



# Multi-Harmonic Cavity for Suppressing Surface Pulsed Heating

Y. Jiang<sup>1, a)</sup> and J.L. Hirshfield<sup>1, 2</sup>

<sup>1</sup>*Yale University, New Haven, CT 06520, USA*

<sup>2</sup>*Omega-P, Inc, New Haven, CT 06511, USA*

<sup>a)</sup> Corresponding author: yong.jiang@aya.yale.edu

**Abstract.** Multi-harmonic accelerating cavities that are explicitly designed for suppressing surface pulsed heating are described. The fundamental TM<sub>010</sub> and its higher harmonic mode of the cavities are to be excited coherently by an external dual frequency RF source in the expectation of lowering surface pulsed heating, so as to reduce breakdown probability and possibly achieve an increase in acceleration gradient.

## INTRODUCTION

In this paper, microwave cavities that support the superposition of the fundamental TM<sub>010</sub> mode and at least one more mode whose eigen-frequency is a harmonic of the TM<sub>010</sub> eigen-frequency are described. RF breakdown appears to be a major hurdle preventing accelerator structures from reaching high gradients. This paper describes experiments being built using multi-harmonic bimodal cavities to systematically study several mechanisms which seem likely to influence the onset of RF breakdown. By deepening the understanding of these mechanisms through the experiments described here, it may lead to improved design of accelerator structures with higher gradient and lower breakdown probability than can be built at present.

In particular, two phenomena provide the main motivation for introduction of a 2<sup>nd</sup> mode at a harmonic frequency. The first phenomenon is the suppression of field emission due to the *anode-cathode effect* [1, 2]. In a longitudinally *asymmetric* cavity [1, 2], phase-locked two-frequency operation with the 2<sup>nd</sup> mode at a frequency double that of the fundamental, can allow the electric field pointing into one wall (cathode-like) to be significantly smaller than the field pointing out of that wall (anode-like), as shown in Fig. 1(a) and (b). A strong anode field will raise the work function barrier to suppress field and secondary emission. The specific design of multi-harmonic cavity to make such an effect prominent has been discussed in details in Ref. [1]. The related experimental effort to explore the anode-cathode effect will be pursuit in parallel to the experiment described in this paper. The second phenomenon is the suppression of pulsed heating [3], which is the focus of this paper. To model pulsed heating in a bimodal cavity, we characterize *E*-field superposition as  $E_{total} = (1 - \alpha)E_1 + \alpha E_2$ , where  $E_{1,2}$  is each electric field component normalized to the same acceleration gradient, and  $\alpha$  is the percentage of the 2<sup>nd</sup> mode such that  $E_{total}$  also provides the same acceleration gradient. Similarly, the surface RF *H*-field is  $H_{total} = (1 - \alpha)H_1 + \alpha H_2$ . Pulsed heating temperature rise  $\Delta T$  can then be approximately scaled in terms of  $H_1$  and  $H_2$  as

$$\Delta T \propto (1 - \alpha)^2 \langle H_1^2 \rangle + \alpha^2 \sqrt{f_2/f_1} \langle H_2^2 \rangle + \alpha \langle H_1^2 \rangle [(1 - \alpha)^2 + \alpha^2 \eta^2] \quad (1)$$

where the frequency term  $\sqrt{f_2/f_1}$  is related to the ratio of surface resistivities,  $\eta = \sqrt{(f_2/f_1)^{1/2} \langle H_2^2 \rangle / \langle H_1^2 \rangle}$ , and the cross term averages out over one period. Fig. 1(c) shows quantitatively, due to the quadratic dependence of  $\Delta T$  upon  $\alpha$ , that there is an optimal range of  $\alpha$  such that  $(1 - \alpha)^2 + \alpha^2 \eta^2 < 1$ , which means it is possible to have lower temperature rise with two modes than for a single mode alone, while maintaining the same acceleration gradient. The modified Poynting vector  $S_c$  [4], and total required RF power  $P_{tot}$ , also follow a quadratic dependence on the mode percentage  $\alpha$ , so use of two modes is expected to lower  $S_c$  and  $P_{tot}$  as well. The reduction of the total required RF power indicates the RF-to-beam efficiency can also be improved with multi-harmonic operation.

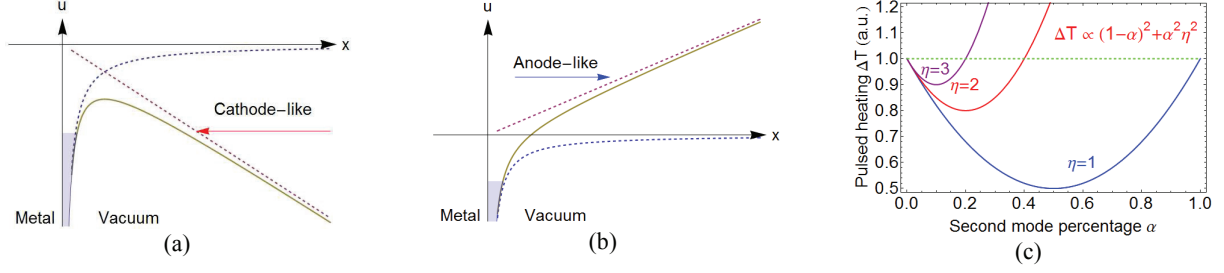
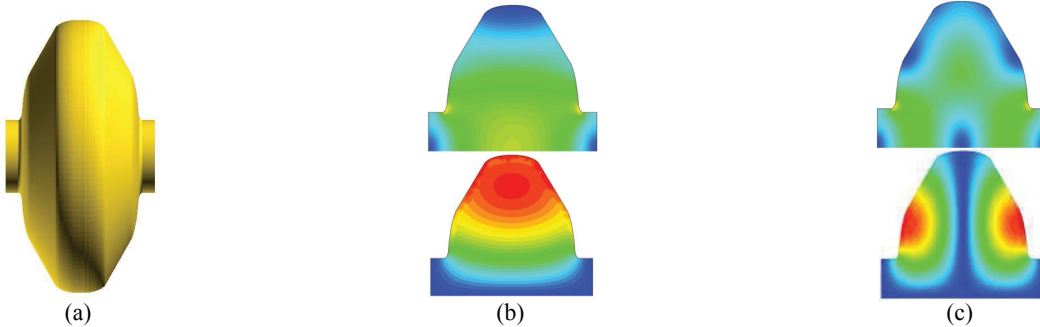


**FIGURE 1.** Potential energy  $u$  of an electron near the surface of a metal with  $x$  the distance from the surface; (a) in an electric field pointing towards the surface (cathode-like), and (b) in an electric field pointing away from the surface (anode-like). (c) Dependence of the surface pulsed heating temperature rise  $\Delta T$  on the 2nd mode percentage  $\alpha$ . There is seen to be a range of  $\alpha$  within which  $\Delta T$  can be smaller than for a single mode (the green dashed horizontal line).

## FEATURES OF $TM_{010}+TM_{011}$ CAVITY

The design concepts of multi-harmonic cavities with field emission and pulsed heating suppression have been described in Ref. [3], which includes one example of a cavity that supports the  $TM_{010}$  mode and a 2<sup>nd</sup> harmonic  $TM_{011}$  mode, and another that supports the  $TM_{010}$  mode and a 3<sup>rd</sup> harmonic  $TM_{012}$  mode. For the latter one, besides the phenomena introduced in the previous section, it is possible to have partial electric field cancellation on walls so that the maximum surface  $E$ -field can be smaller than that of single mode, as another means to suppress field emission. However, the dual-frequency RF source available at Yale would at present only supply multi-MW level of RF power at S-band 2.856 GHz and its second harmonic frequency at C-band 5.712 GHz [1]. Hence the experiment we describe here is for a bi-harmonic cavity operating in first and second harmonic modes. Here we review the design concept and features of  $TM_{010}+TM_{011}$  cavity; the experimental setup will be described in the next section.

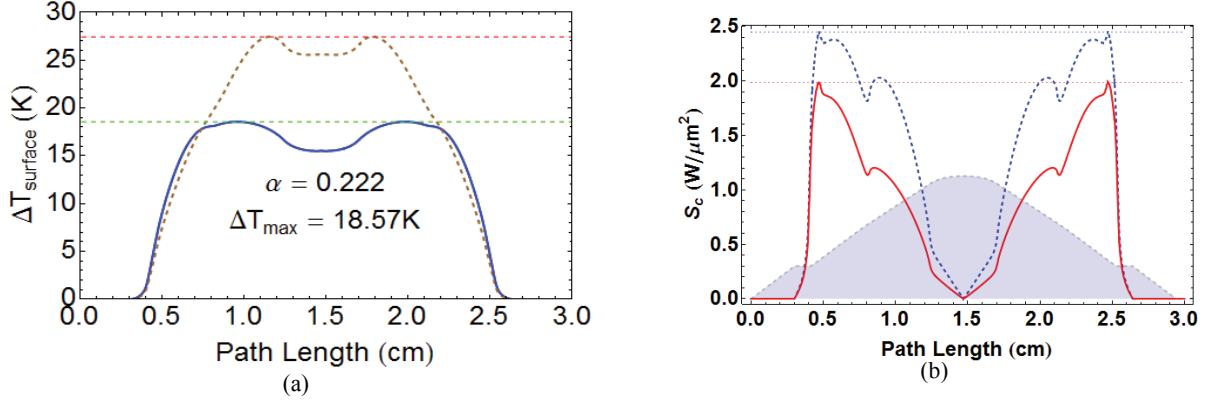
One optimized design for a bimodal cavity supporting the  $TM_{010}$  mode and its 2<sup>nd</sup> harmonic  $TM_{011}$  mode is shown in Fig. 2. It is a full  $\pi$ -mode accelerating cavity, longitudinally symmetric including irises and beam pipes. Its fundamental frequency is at X-band (12 GHz), to benchmark against the empirical criteria recently proposed within the worldwide High Gradient Collaboration: namely, a surface electric field  $E_{sur}^{max} < 260$  MV/m and pulsed surface heating  $\Delta T^{max} < 56$  °K in an X-band structure [4, 5]. The experiment at Yale will utilize a scaled-up version of this cavity design with its fundamental frequency at S-band (2.856 GHz).



**FIGURE 2.** Field patterns in an optimized bimodal cavity (a), for the  $TM_{010}$  mode (b), and its 2<sup>nd</sup> harmonic  $TM_{011}$  mode (c). Top patterns are  $E$ -field, bottom are  $H$ -field.





With this optimized cavity profile, the benefits of reducing surface pulsed heating, modified Poynting vector, and total RF power are shown in Fig. 3 and Table 1. In Fig. 3, the pulsed heating temperature rise for our 2-mode superposition can be 32% smaller than that for the fundamental mode alone for the same cavity; and the maximum modified Poynting vector  $S_c$  can be lower by 20%, with a 22% 2<sup>nd</sup> harmonic component and a relative phase between the two modes of 90° (both modes would be in sychromization should this bimodal cavity be operated in an accelerating structure). The peak surface  $E$ -field is the same as that of the fundamental mode with this phase relationship, and no anode-cathode effect is present. Note that even for a single  $TM_{010}$  mode,  $S_c$  is small due to the reduced  $H$ -field around the iris as a result of optimization. In Table 1, RF parameters of this bimodal cavity are listed in comparison with other cavity configurations. Although the instantaneous surface  $H$ -field is increased, the

pulsed heating temperature rise is lowered since the exposure time to the peak  $H$ -field is shortened, and temperature rise is a time-averaged effect that is quadratically dependent on the mode percentage  $\alpha$  in our 2-mode superposition. The total RF power is reduced, while maintaining the same acceleration gradient, so its effective shunt impedance is significantly increased.



**FIGURE 3.** (a) Optimized maximum pulsed heating temperature rise  $\Delta T$  (blue line) is 18.57 K, compared to that of single mode 27.5 K (brown dotted line), both for a 200 ns pulse width; (b) maximum modified Poynting vector  $S_c$  (red line) is  $1.95 \text{ W}/\mu\text{m}^2$  compared to a single mode value (blue dashed line) of  $2.45 \text{ W}/\mu\text{m}^2$ . The factor  $\alpha$  for the 2<sup>nd</sup> mode in this example is 0.222. The gray area in (b) indicates the stretched cavity profile.

**TABLE 1.** Comparison of RF parameters between an optimized bimodal  $\text{TM}_{010} + \text{TM}_{011}$  cavity and single mode cavities, where effective acceleration gradient is equalized at 100 MV/m, with red/green arrows showing up/down improvements. Pillbox A has the same maximum surface  $H$ -field as that of the fundamental mode in bimodal cavity; Pillbox B the same maximum surface  $E$ -field; and the nose-cone cavity is a single-mode cavity optimized to increase shunt impedance and lower surface pulse heating.

$a/\lambda = 0.12$ $\pi$ mode standing wave effective gradient $E_a = 100 \text{ MV/m}$	 <b>TM<sub>010</sub> + TM<sub>011</sub> Bimodal Cavity</b>			 <b>Pillbox A</b>	 <b>Pillbox B</b>	 <b>Nose-cone</b>
	1 <sup>st</sup> harmonic alone	2 <sup>nd</sup> harmonic alone	78% 1 <sup>st</sup> +22% 2 <sup>nd</sup>	1 <sup>st</sup> harmonic only	1 <sup>st</sup> harmonic only	1 <sup>st</sup> harmonic only
frequency (GHz)	11.9942	23.9884		11.9942	11.9942	11.9942
effective shunt impedance ( $\text{M}\Omega/\text{m}$ )	95.7	38.3	▲131.4	89.7	99.1	113.9
transit time factor	0.765	0.786		0.768	0.753	0.758
max $E_{\text{surf}}$ (MV/m)	246.8	367.4	246.8	209.7	246.8	225.0
max $H_{\text{surf}}$ (MA/m)	0.327	0.634	0.350	0.327	0.298	0.289
max $S_c$ ( $\text{W}/\mu\text{m}^2$ )	2.45	10.3	▼1.95	3.75	3.02	4.20
max $\Delta T$ (K) @ 200ns pulse length	27.5	148.2	▼18.6	27.5	22.87	21.5
wall loss (MW)	1.306	3.263	▼0.95	1.392	1.262	1.097

In addition to their appealing RF properties, multi-harmonic accelerating cavities offer rich features in beam dynamics if an accelerator structure were to be composed of such cavities, because by selectively and coherently exciting synchronized multi-harmonic cavity modes, unconventional spatiotemporal distributions of electromagnetic fields within a cavity can be realized. With two mode superposition, the longitudinal  $E$ -field pattern as function of time can be written as

$$E_{\text{total}} = (1 - \alpha)E_1 \cos \omega t + \alpha E_2 \cos(2\omega t + \phi) \quad (2)$$

where  $\phi$  is the phase of second harmonic relative to the first harmonic. Hence in this dynamical system, there will be two additional parameters, namely second mode percentage  $\alpha$  and relative phase  $\phi$ , compared to the single mode system where  $E_{\text{total}} = E_1 \cos \omega t$ . By varying  $\alpha$  and  $\phi$ , the accelerating field experienced by the head and tail particles relative to the synchronous particle can be engineered to have either a steep slope or a flat top, as shown in

Fig. 4(a). Shown in Fig. 4(b) is the longitudinal phase diagram, with the energy change  $\Delta W$  and phase  $\phi$  relative to that of the synchronous particle. The acceptance in particle phase spread and energy spread can be modified, since the shape of the separatrix in the phase diagram varies as  $\alpha$  or  $\phi$  is changed. Fig. 4(b) shows a scenario where the phase acceptance is widened, yet the energy spread is reduced, as compared the typical *fish* plot for a single mode.

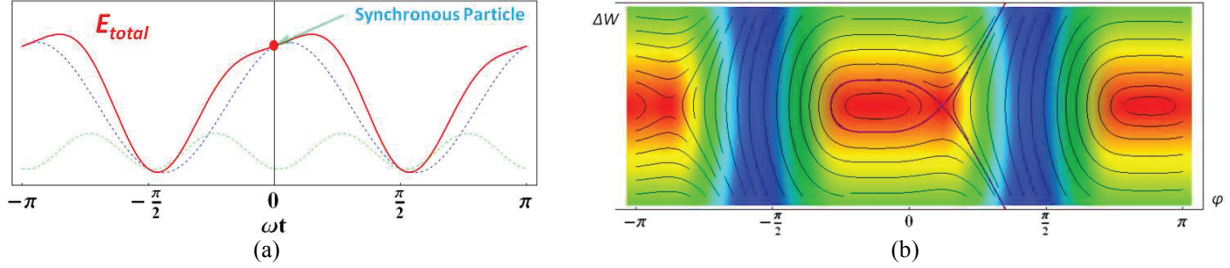


**FIGURE 4.** (a) The longitudinal accelerating  $E$ -field (red solid line) experienced by the synchronous particle in the two-harmonic mode superposition, with the first harmonic (blue dotted) and the second (green dotted). (b) The phase diagram for longitudinal motion, with the energy change  $\Delta W$  and phase  $\phi$  relative to that of the synchronous particle.

## EXPERIMENTAL SETUP

Surface pulsed heating experiments are to be carried out based on availability in the Yale Beam Physics Lab of a unique dual-frequency phase synchronous RF source [1] at S-band (2.856 GHz) and its higher harmonics at C-band 5.712 GHz (possibly X-band 8.856 GHz in the future), as shown in Fig. 5(a). The dual-frequency RF source will provide mutually phase-locked multi-MW  $\sim 1 \mu s$  pulses at both fundamental and higher harmonic frequencies with continuously-adjustable amplitudes and relative phase difference. The cavity geometry suitable for surface pulsed heating and RF breakdown tests at Yale using S-band (2.856 GHz) as the fundamental frequency can be directly scaled from the optimized geometries shown in the previous section.

The technical objective in this experiment is principally to show that the RF breakdown probability and surface damage due to surface pulsed heating can be lower in bimodal cavities than in corresponding conventional single-mode cavities at the same level of acceleration gradient. The intended future outcome is the evolution of a viable cavity design and a structure that can support an effective acceleration gradient  $>150$  MV/m with a breakdown probability that would, in a working accelerator structure, correspond to  $<10^{-7}$  m $^{-1}$  per RF pulse (i.e., one breakdown event per meter structure length per 24-hour day with a 120 Hz pulse repetition rate). Proof-of-principle experiments to be conducted are to involve excitation of the breakdown test structure containing the bimodal test cell, and study of its RF breakdown and surface pulsed heating properties. A schematic of the experimental setup to measure pulsed temperature rise and register RF breakdown events is shown in Fig. 5(b). Because the electrical resistivity depends on the surface temperature, the cavity  $Q$  will change when the cavity surface is heated during high-power pulsing. By exciting a diagnostic mode at a frequency different from the high power sources to reach steady state using another lower power RF source, the coupling to the diagnostic mode will change if cavity  $Q$  is changed. By measuring the change in the amplitude and phase of the reflected power from the diagnostic mode using IQ demodulator to determine the dynamic  $Q$  change, the temperature rise on the certain area of the cavity surface can be deduced based on simulated field pattern of this diagnostic mode. Beam pipe openings of the mode launchers or small openings on the test cell wall can serve as the diagnostic port. Instantaneously excessive reflected power can be registered as the occurrence of RF breakdown. For a test cavity with a 5.2 cm cavity length (equivalent to  $\pi$  phase advance in an S-band accelerator structure), it will take about three days @ 24 hour/day at a 10 Hz rate to accumulate RF breakdown probability for comparison to  $10^{-5}/m$ . Variations in the cavity  $Q$  can indicate long-term degradation to determine permanent surface damage. Visual inspection and SEM examination after high power tests can reveal the location and seriousness of surface damage. RF breakdown tests in travelling wave or standing wave single cell structures [6] can be devised to benchmark with existing RF breakdown data [4]. With better understanding of RF breakdown physics supported by experimental evidence, design concepts for accelerator structures comprising multi-harmonic cavities should emerge from this work.

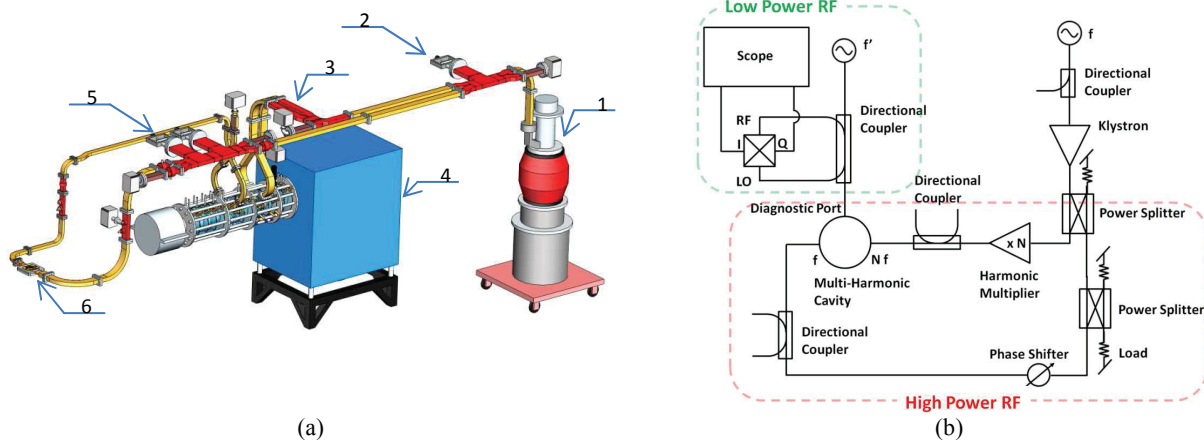


**FIGURE 5.** (a) The RF circuit of two-frequency phase-synchronous source with second harmonic multiplier embedded inside the magnetic flux cage, where item **1** is a 24-MW XK-5 S-band klystron, **2** is a power splitter, **3** is a 3-dB hybrid, **4** is a 300-kV electron gun tank, **5** is a power splitter and phase shifter, and **6** is a bimodal test cell. (b) Experimental schematic of pulsed heating experiment composed of a high power RF section and a low power one.

## CONCLUSION

By selectively exciting synchronized multi-harmonic cavity modes driven externally in a precisely-controlled manner from the dual-frequency RF source available at Yale, unconventional spatiotemporal distributions of electromagnetic fields within a cavity can be realized, with the potential to suppress pulsed heating or field emission at a given level of acceleration gradient; these effects are believed to be precursors to RF breakdown. It is anticipated that deepened understanding of these mechanisms, perhaps through studies of the sort described here and Ref. [1], could lead to improved design of warm structures with higher accelerator gradient and lower breakdown probability than can be built at present.

## ACKNOWLEDGMENTS

The authors would like to thank Professor R.M. Jones from Manchester Univ. (UK) for valuable discussions, and thank Department of Energy for funding support.

## REFERENCES

1. Y. Jiang, S.V. Kuzikov, S.Yu. Kazakov, and J. L. Hirshfield, *Nucl. Instr. Meth. Phys. Res. A*, v657, pp 71-77 (2011).
2. S.V. Kuzikov, S.Yu. Kazakov, Y. Jiang, and J. L. Hirshfield, *Phys. Rev. Lett.*, 104, 214801 (2010).
3. Y. Jiang and J. L. Hirshfield, Proceedings of NA-PAC2013, Pasadena, CA, WEPMA28, pp.1040-1042 (2013).
4. A. Grudiev, S. Calatroni, and W. Wuensch, *Phys. Rev. ST Accel. Beams*, 12, 102001 (2009); and citations therein.
5. A. Grudiev and W. Wuensch, Proceedings of LINAC08, Victoria, Canada, THP062, pp.923-935 (2008).
6. V. A. Dolgashev, S. G. Tantawi, and C. D. Nantista, SLAC-PUB-10667 (2004).